

Citation for published version:

Anderson, C, Khan, MAF, Wong, F, Solovieva, T, Oliveira, NMM, Baldock, RA, Tickle, C, Burt, DW & Stern, CD 2016, 'A strategy to discover new organizers identifies a putative heart organizer', *Nature Communications*, vol. 7, 12656. <https://doi.org/10.1038/ncomms12656>

DOI:

[10.1038/ncomms12656](https://doi.org/10.1038/ncomms12656)

Publication date:

2016

Document Version

Publisher's PDF, also known as Version of record

[Link to publication](#)

Publisher Rights

CC BY

University of Bath

Alternative formats

If you require this document in an alternative format, please contact:
openaccess@bath.ac.uk

General rights

Copyright and moral rights for the publications made accessible in the public portal are retained by the authors and/or other copyright owners and it is a condition of accessing publications that users recognise and abide by the legal requirements associated with these rights.

Take down policy

If you believe that this document breaches copyright please contact us providing details, and we will remove access to the work immediately and investigate your claim.

ARTICLE

Received 2 May 2016 | Accepted 19 Jul 2016 | Published 25 Aug 2016

DOI: 10.1038/ncomms12656

OPEN

A strategy to discover new organizers identifies a putative heart organizer

Claire Anderson¹, Mohsin A.F. Khan^{1,*†}, Frances Wong^{2,*}, Tatiana Solovieva¹, Nidia M.M. Oliveira¹, Richard A. Baldock³, Cheryll Tickle⁴, Dave W. Burt² & Claudio D. Stern¹

Organizers are regions of the embryo that can both induce new fates and impart pattern on other regions. So far, surprisingly few organizers have been discovered, considering the number of patterned tissue types generated during development. This may be because their discovery has relied on transplantation and ablation experiments. Here we describe a new approach, using chick embryos, to discover organizers based on a common gene expression signature, and use it to uncover the anterior intestinal portal (AIP) endoderm as a putative heart organizer. We show that the AIP can induce cardiac identity from non-cardiac mesoderm and that it can pattern this by specifying ventricular and suppressing atrial regional identity. We also uncover some of the signals responsible. The method holds promise as a tool to discover other novel organizers acting during development.

¹Department of Cell and Developmental Biology, University College London, Gower Street, London WC1E 6BT, UK. ²Department of Genomics and Genetics, The Roslin Institute, University of Edinburgh, Easter Bush, Midlothian, EH25 9RG Scotland, UK. ³Biomedical Systems Analysis Section, MRC Human Genetics Unit, IGMM, University of Edinburgh, Crewe Road, Edinburgh, EH4 2XU, UK. ⁴Department of Biology & Biochemistry, University of Bath, Bath BA2 7AY, UK. * These authors contributed equally to this work. † Present address: Heart Failure Research Center, Academic Medical Center, Meibergdreef 15, 1105 AZ Amsterdam, Netherlands. Correspondence and requests for materials should be addressed to C.D.S. (email: c.stern@ucl.ac.uk).

Organizers are formally defined as signalling regions, unique in being able both to induce and to pattern adjacent tissue¹. The dorsal lip of the blastopore, which can induce a complete secondary axis in amphibian embryos, was the first organizer to be discovered, in 1924 (ref. 2). Given the complexity of the vertebrate embryo, one might expect that many organizers should exist, but only a few others have been described³: Hensen's node (the amniote equivalent of the dorsal lip of the blastopore, which can induce and pattern the central nervous system)⁴, the notochord/floor-plate (which can induce and organize different sets of neurons in the neural tube)⁵, the zone of polarizing activity (ZPA, which can induce a patterned set of limb elements)⁶ and the midbrain–hindbrain boundary (isthmus, which can specify and pattern the adjacent regions of the midbrain/tectum and hindbrain/cerebellum)⁷. One reason why so few organizers have been found could be that their discovery requires grafting appropriate tissues at the right time and place, and there are too many possible combinations.

It has been shown that in some cases organizers can substitute for each other. Most strikingly, a graft of Hensen's node from an early (primitive streak stage) embryo into the anterior limb bud of a much later embryo can mimic the action of the limb organizer, the ZPA, by inducing and patterning a full set of skeletal elements including the digits⁸. This raises the intriguing possibility that organizers may share a genetic signature ('synexpression') that confers them with inducing and patterning properties. If this is the case, we should be able to use this genetic signature to point to potential new organizing regions. In this study, we tested this idea by comparing the transcriptomes of three known amniote organizers (Hensen's node, the notochord/floor-plate and the ZPA). This defines a synexpression set of 48 transcripts that are either enriched or depleted in organizers, which we then used to explore the embryo for other regions of synexpression. This suggested that the endoderm of the anterior intestinal portal (AIP) might be a new organizer. The AIP is an endodermal invagination appearing with the head-fold, which moves caudally down the embryo to form the foregut⁹. As it does so, it is closely associated with the developing heart tube. We therefore performed a series of experiments to test whether the AIP can act as an organizer of the heart. Ablation and transplantation experiments *in vivo*, along with co-culture *in vitro*, revealed that the AIP endoderm can induce heart fate from non-cardiac mesoderm as well as pattern the heart field by specifying ventricular and suppressing atrial regional identity.

Results

Defining a gene signature for organizers. To investigate whether organizers have a common genetic signature of enriched and depleted transcripts, we designed a differential microarray screen in chick embryos, comparing three known organizers to their most similar non-organizer tissue. First, we chose stage (HH¹⁰) 3⁺/4 Hensen's node, which induces and patterns the neural plate¹¹, compared with the posterior primitive streak, which cannot (Fig. 1a). We also sampled the later node (HH6), which has lost its ability to induce a full neural plate¹¹. This three-way comparison was designed to reveal transcripts associated with full organizer function. Second, we selected the notochord and floor-plate at HH10–11, responsible for organizing the dorso-ventral axis of the neural tube⁵, and compared this to the dorsal neural tube (Fig. 1b). Finally, we compared the posterior wing bud, containing the ZPA⁶, to the anterior wing bud at HH20–21 and HH24 (Fig. 1c). Each comparison generated a list of transcripts significantly enriched or depleted in that organizer (≥ 1.2 -fold the \log_2 of the expression level, and a false discovery rate ≤ 0.05). The dataset was submitted to ArrayExpress with the

title 'Microarray analysis of chick embryonic tissues: gastrulation, neural tube/notochord and limb development' and given accession number E-MTAB-4048). These lists were then combined using a Boolean algorithm to find enriched or depleted transcripts common to all three organizers. This approach uncovers relative changes in expression between

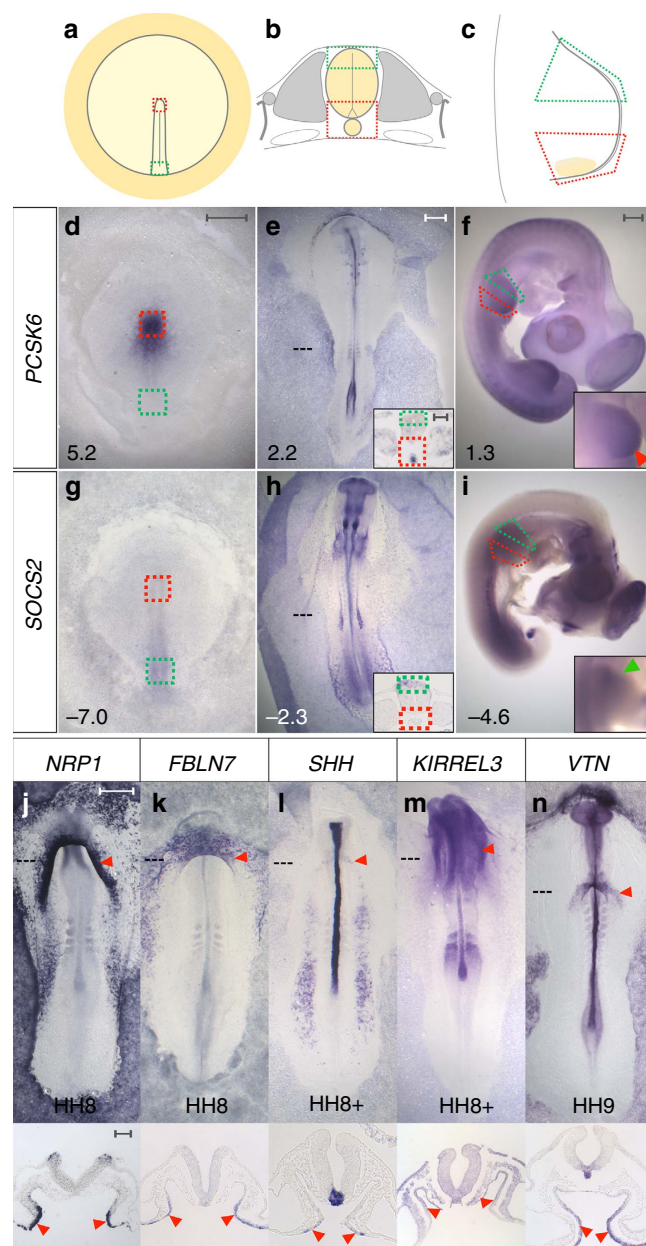


Figure 1 | Transcriptome comparison of known organizers reveals genes co-expressed in organizers and in the Anterior Intestinal Portal endoderm. (a–c) Experimental design. (a) Hensen's node (red box) was compared with posterior primitive streak (green box); (b) notochord and ventral neural tube (red box) was compared with dorsal neural tube (green box) and (c) posterior wing bud (red box) was compared with anterior wing bud (green box). (d–i) One gene enriched in organizers is *PCSK6* (d–f, red boxes, red arrowhead in f-inset) and *SOCS2* exemplifies a depleted gene (g–i, green boxes, green arrowhead in i-inset). Fold-change values are indicated. (j–n) Examples of organizer-enriched transcripts expressed in the anterior intestinal portal endoderm (AIP) (red arrowheads): *NRP1* (j), *FBN1* (k), *SHH* (l), *KIRREL3* (m) and *VTN* (n). Scale bars, 0.5 mm in whole-mounts and 0.1 mm in sections.

organizer cells and neighbouring regions, even if the absolute level of expression is widely different at different stages: a putative organizer gene set of 31 enriched and 17 depleted transcripts is revealed (Supplementary Fig. 1a–d and Supplementary Data 1). Interestingly, over 60% of the enriched genes encode membrane-associated or secreted molecules and 7% represent transcription factors, whereas transcription factors are much more frequent (38%) among the depleted genes (Supplementary Fig. 1c). One possible interpretation of this is that the synexpression set is enriched for signalling molecules emitted by the organizer and depleted of transcriptional repressors that suppress the organizer state.

The AIP endoderm as a candidate organizer. Next, we used this set to verify the expression of the selected genes (Fig. 1d–i, Supplementary Figs 2 and 3), as well as to explore whether the synexpression signature occurs in other places and stages during development. A large-scale *in situ* hybridization analysis of the 48 genes was undertaken from pre-primitive streak stage up to HH27; these expression patterns can be browsed on eChick atlas¹² (www.echickatlas.org). One embryonic region appropriately expresses 35 genes from the organizer gene set: the endoderm of the AIP. At some stage between HH7–14, 20/31 enriched transcripts are detected (Supplementary Fig. 4a–t), 15/17 organizer-depleted genes are appropriately absent from the early AIP (Supplementary Fig. 4u–k), and SOCS2 and BTG2 are absent before HH10 and HH14 respectively (Supplementary Fig. 4l',m'). Thus, the AIP shares a similar transcriptional profile to other known organizers.

There is substantial evidence that the early endoderm adjacent to the bilateral cardiac mesoderm is required for normal heart formation in chick, amphibian and fish embryos^{13,14}, but less is known about the AIP endoderm of later stages. Genetic or manual ablation of the AIP endoderm in mouse and chick embryos results in cardia bifida^{15–19} (failure of the bilateral heart progenitors to fuse in the midline), rotation defects¹⁶ and downregulation of early cardiac genes¹⁵, indicating that a functional AIP endoderm is required for normal heart formation, but its inducing and patterning abilities have not been tested. Could the AIP be an organizer of the heart?

The AIP can induce cardiac identity from non-cardiac mesoderm.

We first confirmed that ablation of the AIP at HH8 does indeed cause cardia bifida and abnormal heart rotation (Supplementary Fig. 5). Next, to test if the AIP can induce cardiac identity, a necessary prerequisite is to identify a suitable responding tissue. Fate and specification maps indicate that the paraxial mesoderm adjacent to Hensen's node at HH5 (prospective head mesoderm) is neither fated nor specified as heart^{20–24}, but is competent to respond to cardiac inducing signals²². We compared this mesoderm (named #3) with four other regions of HH5 mesoderm (Supplementary Figs 6a and 7a): #3 does not contribute to the heart when grafted homotopically (Supplementary Fig. 7b–h), and is the only region of mesoderm that does not express cardiac markers when explanted either *in vitro* (Fig. 2 i,l,o,r,u,x,a',b' and Supplementary Table 1) or in a host embryo (Supplementary Fig. 7j–v and Supplementary Table 2). Mesoderm #3 is therefore suitable for testing whether the early AIP can induce heart fate. The AIP induces early cardiac markers, *MYOCD*, *NKX2.5* (Fig. 2j,m and Supplementary Fig. 8b,c), *GATA4*, *TBX5*, *ISL1* and *MEF2C* in explants of #3-mesoderm (Supplementary Fig. 8d–g), while co-culture with control (Cont.), non-AIP endoderm from the lateral embryo, largely does not (Fig. 2k,n, Supplementary Fig. 8b–h, Supplementary Tables 2 and 3). Strikingly, spontaneous beating is observed after 48 h of *in vitro*

co-culture of #3-mesoderm with AIP (Supplementary Movie 1), but not with control, non-AIP endoderm. Together these results show that the AIP endoderm can induce cardiac identity in mesoderm that is not otherwise fated to become part of the heart.

Patterning by inducing ventricular identity and suppressing atrial character. Many of the known early heart markers are normally expressed in the bilateral cardiac mesoderm before the AIP forms (around stage HH5; Supplementary Fig. 6a–f), whereas regional markers of anterior–posterior heart tube patterning are observed later (after HH9; Supplementary Fig. 6v–n'). Ventricular markers (*VMHC1/MYH15*, *IRX4* and *NPPB*) are initially expressed in the medial splanchnic mesoderm^{25–27} immediately adjacent to the AIP (Supplementary Fig. 6d',f',g'), and the atrial marker *AMHC1* is in the lateral splanchnic mesoderm²⁸ (Supplementary Fig. 6c'). In #3-mesoderm explants cultured either in a host embryo or *in vitro*, AIP induces *VMHC1/MYH15*, *IRX4* and patchy *NPPB* expression (Fig. 2b–d,p,s,v, Supplementary Tables 2 and 3). AIP also induces *GJA5* (Fig. 2e,y), which marks the anterior ventricular myocardium, endocardium and outflow tract (Supplementary Fig. 6h'). AIP does not induce *AMHC1* (Fig. 2f,b') or *SHOX2* (Fig. 2g,e'), a marker of the sinoatrial node (Supplementary Fig. 6i',p'). These results show that the AIP can induce ventricular cardiac identity in mesoderm not destined to this fate.

Previous tissue recombination experiments using HH5–6 chick explants have demonstrated that anterior-lateral endoderm adjacent to the early cardiogenic mesoderm can induce heart gene expression in posterior primitive streak²⁹. Are the induction properties of the HH8 AIP endoderm distinct to the early anterior-lateral endoderm? To test this, we co-cultured HH5 anterior-lateral endoderm with non-cardiac #3-mesoderm (Supplementary Fig. 9a and Supplementary Table 4). Unlike AIP endoderm, anterior-lateral endoderm does not induce ventricular markers (Supplementary Fig. 9b–e) nor does it induce *AMHC1* (Supplementary Fig. 9f). These data show that the anterior-lateral endoderm is different to the AIP endoderm and that the ability to induce ventricular character is a property specific to the AIP endoderm.

To test if the AIP patterns the heart tube by specifying ventricular identity, AIP from transgenic GFP donors was grafted over the cardiogenic mesoderm of a host embryo (Fig. 3a). Strikingly, this expands the expression of *VMHC1/MYH15* and *IRX4* posteriorly into the prospective atrial region (Fig. 3c–l), while expression of the atrial marker *AMHC1* is abolished (Fig. 3m–q). Moreover, the AIP represses *AMHC1* in #1-mesoderm which would normally express it (Fig. 3r–t and Supplementary Table 3); since *IRX4* is known to repress *AMHC1* (refs 26,30), this repression by the AIP may be either direct or indirect, due to prior AIP-mediated induction of *IRX4*. Thus, the AIP not only induces ventricular identity, but also actively blocks atrial character. The ability to induce a new fate in responding tissues and to impart a spatial pattern are properties shared by other known organizers³. Taken together, these results show that the AIP endoderm is distinct from other endodermal regions, in that it can both induce cardiac identity in mesoderm not destined for this fate and also pattern heart mesoderm by promoting ventricular and suppressing atrial regional character.

Common signals between organizers. Grafts of either Hensen's node⁸, notochord or floor-plate³¹ into the anterior limb bud can induce extra digits, suggesting that at least some signals (an obvious one being SHH) may be common to different organizers. We therefore tested whether the heart-inducing or ventricle-specifying functions of the AIP can be mimicked by

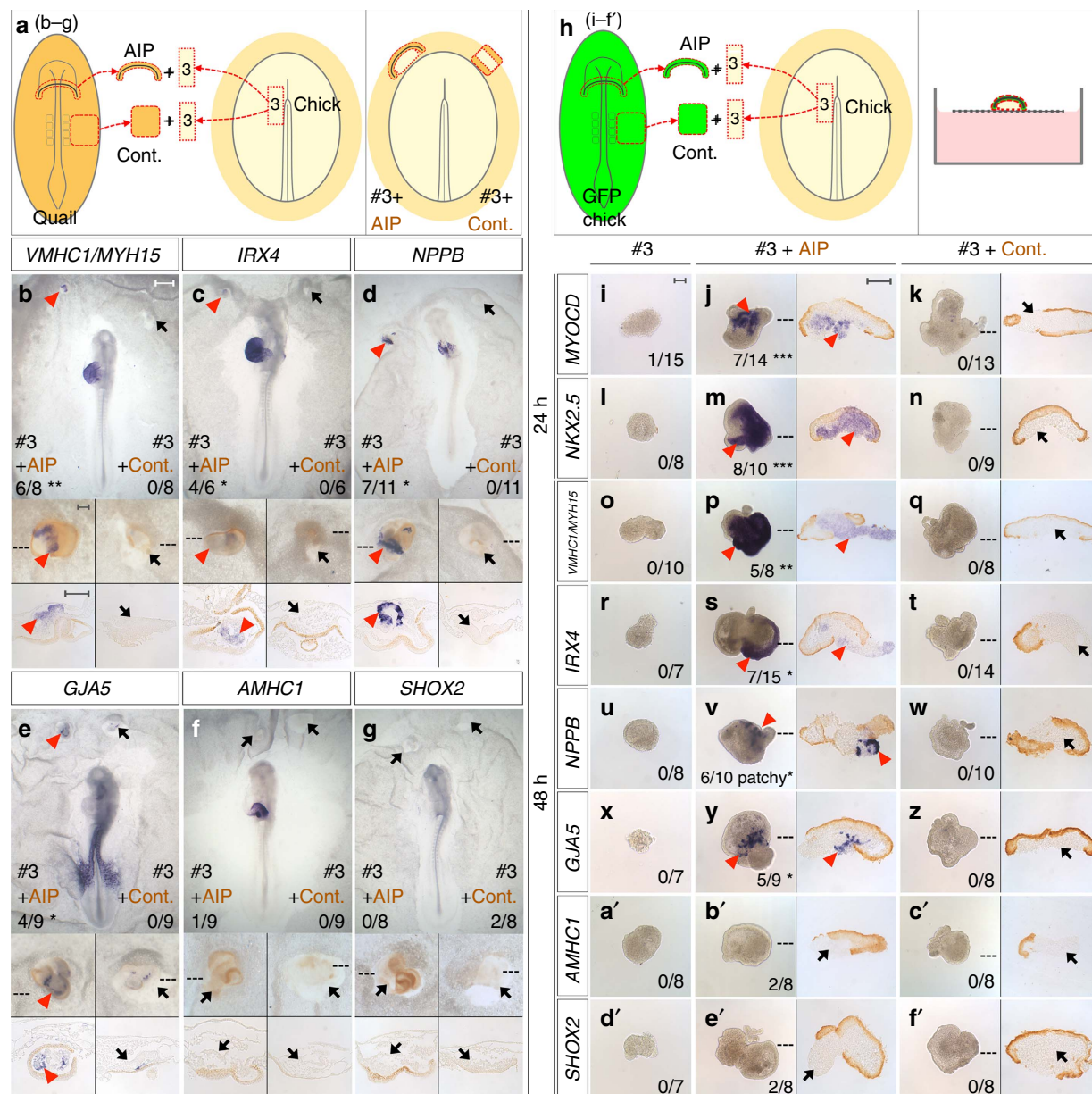


Figure 2 | AIP induces cardiac and ventricular identity in non-cardiac mesoderm. (a) AIP or control (Cont.), lateral endoderm from a HH8 quail co-cultured with anterior-medial mesoderm (#3) from a HH5 chick embryo overnight in the anterior area opaca of a host chick. (b–g) Regional myocardium markers *VMHC1/MYH15* (b), *IRX4* (c), *NPPB* (d) and *GJA5* (e) are induced in #3-mesoderm by quail (brown) AIP (red arrowheads), but not by control endoderm (Cont., black arrows), whereas *AMHC1* (f) and *SHOX2* (g) are not induced (black arrows). (h) *In vitro* co-culture of #3-mesoderm with GFP-AIP (j,m,p,s,v,y,b',e') or -Cont. (k,n,q,t,w,z,c',f') for 24 (j,k,m,n) or 48 h (p,q,s,t,v,w,y,z,b',c',e',f'). No expression is seen in #3-mesoderm cultured alone (i,l,o,r,u,x,a',d'). AIP (brown) induces *MYOCD* (j), *NKX2.5* (m), *VMHC1/MYH15* (p), *IRX4* (s), *NPPB* (v) and *GJA5* (y) in #3-mesoderm (red arrowheads), but Cont. does not (brown, k,n,q,t,w,z, black arrows). Neither *AMHC1* nor *SHOX2* are induced (black arrows) by AIP (b',e') or by Cont. (c',f'). * $P \leq 0.05$, ** $P \leq 0.005$, *** $P \leq 0.0005$ using two-tailed Fisher's exact test. Scale bars, 0.5 mm in whole-mounts and 0.1 mm in insets, explants and sections.

other organizers. We find that Hensen's node induces patchy expression of *VMHC1/MYH15* but not *MYOCD* in #3-mesoderm cultured in a host (Supplementary Fig. 10a,b and Supplementary Table 5), as well as in explants (Supplementary Fig. 10c,d and Supplementary Table 5). Hensen's node has also been shown to induce ectopic *VMHC1*, but not *AMHC1* in the germinal crescent and the lateral plate mesoderm³², comparable to the ability of the AIP to induce ventricular markers. Conversely, to test whether the AIP can mimic the neural inducing activity of Hensen's node, we grafted AIP endoderm into the area opaca³³ at HH3⁺: this induces the early neural marker *SOX3*, but not the later neural

plate marker *SOX2* (Supplementary Fig. 10e,f). Finally, we tested whether the AIP can mimic a ZPA graft into the anterior wing bud: strikingly, the AIP causes duplication of digit-2 (Supplementary Fig. 10h). Therefore, the AIP is partly interchangeable with other organizers at earlier and later stages of development, some of which could be related to its expression of *SHH* (Fig. 11) or *FGF8* (ref. 34). However it seems that the ability of organizers to substitute for each other is limited.

Signals from the AIP endoderm. The inducing and patterning activities of other known organizers rely on multiple signals,

acting together and/or sequentially^{35–37}. FGF8 (refs 38,39) and SHH (refs 40,41) play important roles in other organizers; both have been implicated in cardiogenesis^{34,42} and both are expressed in the AIP. However, our synexpression set contains many other secreted or membrane-associated factors that have not hitherto been implicated either in the activity of other organizers or in cardiac gene induction or heart patterning. Four of these are expressed in the early AIP: *NRP1*, *FBN7*, *KIRREL3* and *VTN* (Fig. 1j,k,m,n). To investigate their activity, we co-cultured #3-mesoderm with pellets of cells transfected with expression plasmids encoding these four factors. This combination partly mimics the AIP, sometimes inducing patchy expression of the

ventricular markers *VMHC1/MYH15* (Fig. 4a) and *NPPB* (Fig. 4b), but not *IRX4* (Supplementary Fig. 11f) or other early cardiac markers (Fig. 4c, Supplementary Fig. 11a–e and Supplementary Table 6).

These results suggest that other signals are required, possibly SHH and FGF8, but also considerable complexity, not unlike other organizers, which are believed to emit different signals at different times to account for their various inducing and patterning functions^{35–37}. Accordingly, some gene expression profiles change over time as the organizer changes its properties. Although HH8 AIP endoderm was used in co-cultures, the AIP continues its developmental programme, expressing transcripts that are detected in the later AIP (Supplementary Fig. 12). HH8 AIP cultured either alone or with #3-mesoderm expresses genes, including those that encode secreted or membrane-associated molecules normally observed in the HH10 AIP (Supplementary Fig. 4j,k), after 24 h (Supplementary Fig. 12a–d) and those expressed in the HH12–13 AIP (Supplementary Fig. 4q,s) after 48 h (Supplementary Fig. 12e–h). These results suggest that the signalling properties of the AIP endoderm mature over the culture period as they do in the embryo.

Taken together, our results implicate the AIP as an organizer of the heart, and suggest that a complex combination of signals account for its heart inducing and patterning functions at early stages of heart tube formation.

Discussion

Our results suggest that organizers do share a common genetic signature, and that this property can be used to identify putative new organizers acting during development. The choice of the three organizers to compare was relatively arbitrary and perhaps we should have used a different well-characterized organizer, the mid-hindbrain boundary (MHB) or isthmus organizer^{3,7} instead of the comparison between notochord/floor-plate with dorsal neural tube (particularly as the latter is also a signalling region). The main reason why we did not use the MHB is that it is difficult

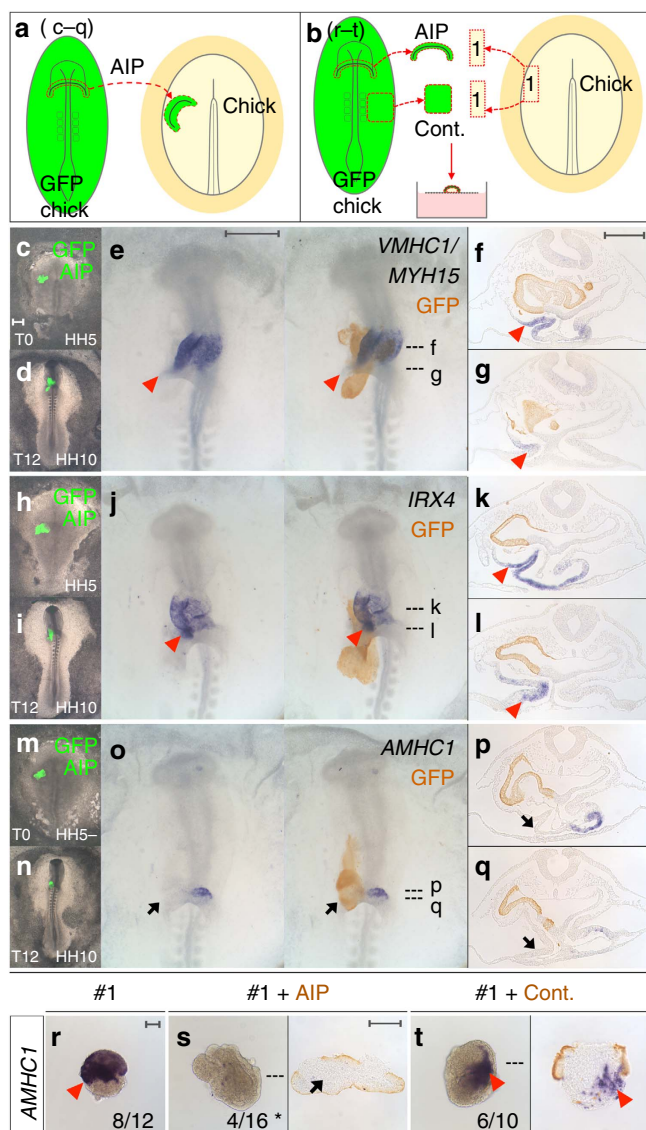


Figure 3 | AIP specifies ventricular regional identity and represses atrial character. (a) AIP (green, c,d,h,i,m,n; brown, e-g,j-l,o-q) from a HH8 GFP chick was grafted heterotopically onto cardiogenic mesoderm of a HH5 wild-type chick host (c,h,m, T0) and grown for 12 h (d,i,n, T12). (c–q) AIP expands *VMHC1/MYH15* (e–g) and *IRX4* (j–l) expression (red arrowheads) and abolishes *AMHC1* (o–q, black arrows). (b) *In vitro* co-culture of #1-mesoderm from a HH5 chick with HH8 GFP-AIP or control (Cont.) endoderm (brown) for 48 h. *AMHC1* expression in #1-mesoderm (r, red arrowhead). AIP represses *AMHC1* in #1-mesoderm (s, black arrow), Cont. does not (t, red arrowhead). * $P \leq 0.05$ using two-tailed Fisher's exact test. Scale bars, 0.5 mm in whole-mounts and 0.1 mm in explants and sections.

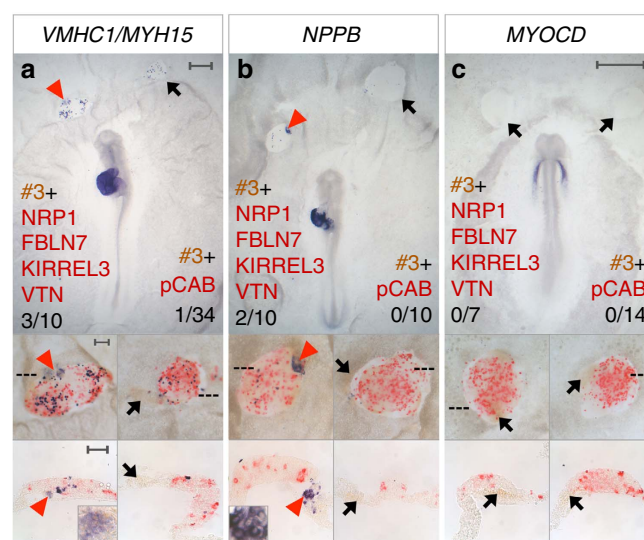


Figure 4 | Secreted molecules induce ventricular markers. (a–c) HH5 quail (brown) #3-mesoderm co-cultured in a chick host with cell pellets transfected with *NRP1* + *FBN7* + *KIRREL3* + *VTN* (red) either overnight (a,b) or for 6–9 h (c). *VMHC1/MYH15* and *NPPB* are induced in #3-mesoderm (a,b, red arrowheads) but *MYOCD* is not (c, black arrows). Control pellets (red; pCAB) do not induce *VMHC1/MYH15*, *NPPB* or *MYOCD* (a–c, black arrows). Scale bars, 0.5 mm in whole-mounts and 0.1 mm in insets and sections.

to identify a non-organizer tissue that is similar enough to this boundary in every other respect. The organizer gene set could be refined further using this tissue in future. Nevertheless, this study is an important proof of principle and, based on the synexpression of 48 genes, we uncover the AIP endoderm as a putative organizer because it can both induce cardiac identity and pattern the heart field by specifying regional characteristics (inducing ventricle and suppressing atrial character).

Previous studies have concluded that the endoderm is required for heart development (reviewed in ref. 13). Many of these studies investigated the early anterior-lateral endoderm adjacent to the cardiac mesoderm at HH4–6 (refs 34,43–48). Tissue recombination experiments have shown that this endoderm can reprogram non-cardiac tissues to heart identity²⁹ and BMPs, FGFs and inhibition of WNT signalling have been implicated in this^{13,22,32,34,49–53} (Fig. 5a). Some recombination experiments have used posterior primitive streak or posterior lateral plate (#4–5; Supplementary Figs 6a and 7a) explants as a responding tissue to test for cardiac induction^{29,49,50,53}. However, it has since been shown that these tissues express *MYOCD* (ref. 43), *GATA* (ref. 54) and *TBX20* (ref. 14) transcription factors, and can express *MYOCD* and *VMHC1/MYH15* following culture *in vitro* (Supplementary Table 1) leaving open the possibility that these experiments do not demonstrate a true change of fate in this tissue. Widespread expression of some early cardiac markers makes it difficult to find a responding tissue suitable for an induction assay (neither being fated to give rise to heart nor express any of the markers being assessed as a result of the induction). Here we use anterior-medial mesoderm (#3), which is neither fated nor specified as heart^{20–24} and can be used to assess both induction and patterning rigorously.

The expression patterns of early cardiac markers, like *NKX2.5* (ref. 29), and the signalling molecules previously implicated in their induction (*BMP2/4/7* (ref. 22), *FGF8* (ref. 34) and *CRESCENT* (ref. 49)) indicate that initial signals act at an early stage of cardiogenesis (HH4–6, Fig. 5a) before the AIP forms. Our

results show that the AIP from a later stage embryo can also induce heart identity (reprogramming non-heart #3-mesoderm from an earlier stage donor) as well as pattern it by specifying ventricular and suppressing atrial character. During normal development, the AIP is likely to be responsible for the later patterning functions (Fig. 5b), but our results show that it can also mimic the activity of earlier endoderm. This could be due to the presence of AIP precursors within this early endoderm^{21,55,56} and the continued expression of *BMP2* (ref. 22) and *FGF8* (ref. 34). This is reminiscent of other organizers, for example, Hensen's node can initiate the entire process of neural induction, even though the first neural inducing signals begin before gastrulation, long before Hensen's node can be defined³⁸. This could be a general feature of organizers, perhaps because they produce many signals. However, the signals emitted by organizers also change over time as their patterning properties evolve, which is seen in organizers like Hensen's node^{11,36}, as well as in the AIP.

Heart progenitor cells become determined to either the ventricular or atrial compartment at around HH8 (refs 28,57,58), consistent with the timing of signals from the AIP endoderm that induce ventricular and repress atrial character (Fig. 5b). Retinoic acid signalling from the posterior lateral plate mesoderm is known to control the allocation of cardiac progenitor cells to the atrial lineage^{28,57,59}. We have shown that signals from the AIP endoderm, *NRP1*, *FBN1*, *KIRREL3* and *VTN* when combined can sometimes induce *VMHC1/MYH15* and *NPPB* (Fig. 5c), but whether these signals also repress atrial identity remains to be tested. *BMP2/4*, *FGF4* and Wnt inhibitors have also been shown to induce *VMHC1* (refs 22,32,49), although the results of these studies do not rule out induction of heart identity rather than regionalization. Additional regional markers need to be tested to resolve this. Interestingly, both *VTN* and *NRP1* have other, much later roles in heart patterning.

There is conflicting evidence about the extent to which cells that make up the AIP roll around it (involution) and turn over rapidly, or whether they remain in place as it advances caudally

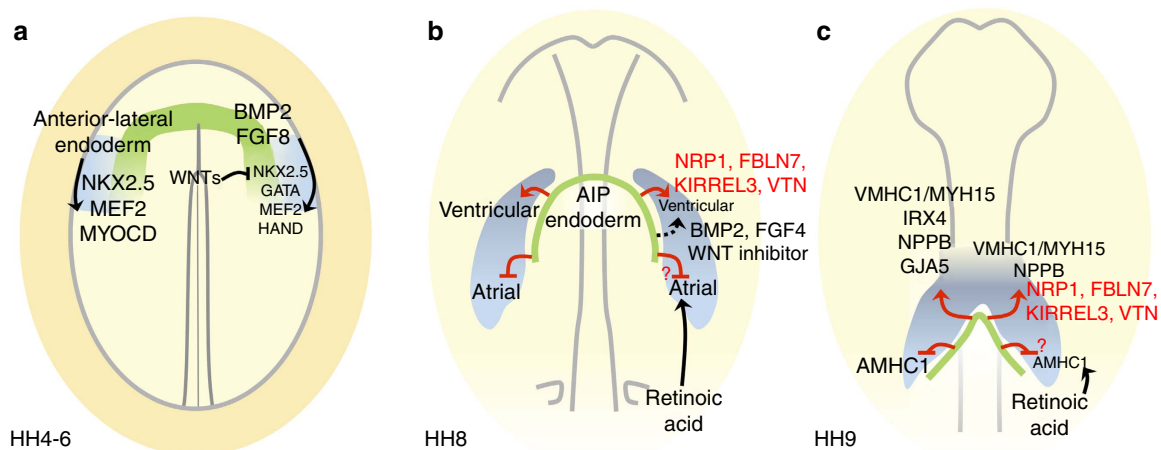


Figure 5 | Successive roles of the endoderm in heart induction and patterning. Each diagram represents a stage in development; in each, tissue interactions are depicted on the left, signals on the right. (a) Initially (HH 4–6), the anterior-lateral endoderm (including some prospective AIP⁵⁶, green) is required for the adjacent cardiac mesoderm (light blue) to express *NKX2.5*, *MEF2C*²⁹ and *MYOCD*⁴³. *BMP2* and *FGF8* signalling from the anterior-lateral endoderm induce *NKX2.5*, *GATA*, *MEF2* and *HAND* transcription factors^{22,34,51,52}. The anterior endoderm expresses WNT inhibitors including *Cresemb*, which can induce *NKX2.5* (ref. 49). (b) At HH8, progenitor cells are becoming determined as either atrial or ventricular^{28,57,58}. The AIP endoderm induces ventricular character and represses atrial identity. Signals from the AIP endoderm, including *NRP1*, *FBN1*, *KIRREL3* and *VTN* described here (red text and arrows) and previously reported *BMP2*, *FGF4* and Wnt inhibitors^{22,32,49} (black text and arrows), induce some ventricular markers, which are integrated with atrial-inducing retinoic acid signalling from the posterior lateral plate mesoderm^{28,57,59}. The signals from the AIP endoderm that repress atrial identity are unknown. (c) At HH9, when regional markers of anterior-posterior heart tube patterning begin to be expressed, AIP endoderm induces ventricular markers *VMHC1/MYH15*, *IRX4*, *NPPB* and *GJA5* (the latter expressed from HH12) and represses the atrial marker *AMHC1*. Four secreted molecules from the AIP endoderm, *NRP1*, *FBN1*, *KIRREL3* and *VTN* can induce *VMHC1/MYH15* and *NPPB*.

down the embryo^{19,55,60}. Neither possibility is incompatible with the AIP being an organizer. The cellular composition of Hensen's node constantly changes as cells move in and out of it⁶¹ but it also contains resident cells⁶² and similar findings have been made for the ZPA of the limb⁶³. In all these cases the organizer property, as well as molecular markers for it, remain in the region rather than moving with the cells: cells regulate their expression and functional properties according to their current position⁶¹. These findings raise the general principle that organizers define a position within the embryo where a set of properties come together. Using a 'synexpression' gene set for this state should not only allow us to seek new organizers, but also to investigate the clues that instruct cells to have such properties in particular places in the embryo.

Our novel approach of identifying genes common to different organizers offers great potential not only for uncovering new organizing centres during development, but also as a tool to identify new signalling molecules underlying organizer function, as well as transcription factors that confer cells with this property. Interestingly, we find that the synexpression set is enriched for signalling molecules (15 of the 31 enriched genes), whereas transcription factors are more abundant among the depleted genes (6/17), suggesting that some transcriptional repressors may function to suppress the organizer state in non-organizer tissues.

Methods

Differential microarray screen and analysis. Fertile Brown Bovan Gold hens' eggs (Henry Stewart, UK) were incubated at 38 °C and staged according to Hamburger and Hamilton (HH)¹⁰. The following tissues were collected (three separate samples of each) and RNA extracted by standard methods: Hensen's Node at HH3⁺/4 (HH4 HN) and HH5/6 (HH6 HN), posterior primitive streak at HH3⁺/4 (HH4 PS), HH10/11 notochord and adjacent ventral neural tube/floor-plate (VNT) and the corresponding dorsal neural tube (DNT), the posterior third of the limb at HH20/21 (HH20 PL) and HH24 (HH24 PL) and the anterior third of the limb at HH20/21 (HH20 AL) and HH24 (HH24 AL)⁶⁴.

Hybridization to Affymetrix microarrays was conducted by ARK-Genomics at the Roslin Institute, University of Edinburgh, as described in the Affymetrix GeneChip Expression Analysis Technical Manual (Affymetrix, Inc.). Briefly, 15 µg of total RNA from each sample was reverse-transcribed using a T7-oligo (dT) primer in the first-strand complementary DNA (cDNA) synthesis. After RNAase-H treatment, second-strand cDNA synthesis was carried out. The cDNA was then purified and used as a template in the subsequent *in vitro* transcription reaction for linear amplification of each transcript, and incorporation of biotinylated CTP and UTP using T7 RNA polymerase. The biotinylated cRNA targets were fragmented and hybridized to the Affymetrix GeneChip Chicken Genome Array, which provides good coverage of the chicken genome (32,773 transcripts corresponding to over 28,000 genes). Twenty-seven arrays were used in total (samples from 9 tissues, each in triplicate). Hybridization was performed at 45 °C for 16 h with constant rotation (60 rpm). The microarrays were then automatically washed and stained with Streptavidin-phycoerythrin conjugate (SAPE; Invitrogen) in a GeneChip fluidics station (Affymetrix). Fluorescence intensities were measured with a GeneArray scanner 3,000 (Affymetrix). The scanned images were analysed as described in the Affymetrix GeneChip Command Console 3.0 User Manual.

Gene expression data generated from the GeneChip software (GCOS) were normalized using the probe logarithmic intensity error (PLIER) method⁶⁵ within the Affymetrix Expression Console software package. The normalized data were then analysed using the Limma and FARMs⁶⁶ packages within R in Bioconductor. Venn diagrams were generated using the R package Vennr with dependencies, graph, RGL, gplots, gtools and reshape. Weights used for scaling the Venn diagrams were based on a priori count data reflecting intersections of genes between different comparisons of datasets.

Dataset comparisons. Pair-wise comparison of samples was performed as follows:

HH4 HN versus HH4 PS;
HH6 HN versus HH4 PS;
HH4 HN versus HH6 HN;
VNT versus DNT;
HH20 PL versus HH20 AL;
HH24 PL versus HH24 AL.

Probes with a fold change (FC) ≥ 1.2 (log₂) and a false discovery rate ≤ 0.05 were deemed significant. The results of these individual comparisons (using significant enrichment or depletion as the indicator, rather than absolute amounts) were then combined using the Boolean algorithm: ((HH4 HN versus HH4 PS AND

(HH4 HN versus HH6 HN) OR HH6 HN versus HH4 PS)) AND VNT versus DNT AND (HH20 PL versus HH20 AL OR HH24 PL versus HH24 AL). Probes that are differentially enriched or depleted significantly in this algorithm comprise the organizer gene set. The first set of comparisons selects genes enriched or depleted in the early (HH3⁺/4) Hensen's node compared with the posterior streak, some of which remain expressed the same way at the later (HH5/6) stage. The comparisons for the limb select genes enriched or depleted in the posterior limb bud (containing the ZPA) at either HH20/21 or HH24.

The dataset was submitted to ArrayExpress with the title 'Microarray analysis of chick embryonic tissues: gastrulation, neural tube/notochord and limb development' and given accession number E-MTAB-4048.

Embryo manipulation. Fertilized Brown Bovan Gold hens' eggs (Henry Stewart, UK), Coturnix coturnix japonica quails' eggs (B.C. Potter, Rosedean Farm, UK, and Blue Bridge Engineering Limited, Essex, UK) and transgenic GFP chicken eggs⁶⁷ (Roslin Institute, Edinburgh, UK) were used. Embryo manipulations were performed in Pannett-Compton saline and modified New culture^{68,69}. Tissues were excised from donor embryos using 0.12% w/v trypsin (porcine trypsin 1:250, Sigma) in Pannett-Compton saline and 30 G syringe needles, washed with saline and kept on ice until needed. Mesoderm (#1–5, from both the left and the right sides and used randomly) was harvested from HH5[−] to HH5⁺ donor embryos. Early AIP endoderm (AIP) and control (Cont.) lateral endoderm (the endoderm underlying the somites and proximal lateral plate mesoderm) were harvested from HH8[−] to HH8⁺ embryos. Early AIP endoderm was used because cardiac progenitors are closely associated with the AIP at this time, and because it is easier to isolate the AIP at this stage than later, when the heart is beating. Anterior-lateral endoderm (#1–2E) and anterior-medial endoderm (#3E) were harvested from HH5 donor embryos. Host embryos ranged from HH4⁺ to HH6. Grafts were placed on the left or the right side of host embryos; no differences were noted in the results. After grafting, the embryos were incubated for either 6–9 h or overnight (12–18 h). Limb grafts were performed *in ovo* at HH20–21 and incubated for 5 days⁷⁰.

Delivery of factors using transfected cells. Chicken *NRP1* (NM_204782.1; F primer CCGCTCTCGGAAGG, R primer CATCCGATTCTCTG), *FBLN7* (XP_003640934.1, formerly *FIBULIN 7-LIKE*; F primer GGAC-CATGGCTTCGGGGCTC, R primer CCTGGTCTGCCCTAGAACTCATAGGC), *VTN* (NM_205061.1; F primer CTCTGGATCCTGCTCAGTCACAGTAG with introduced BamHI site, R primer CTGGCGGTGAATTCGGGTCTAGC with introduced EcoRI site) and *KIRREL3* (XP_004948018.1; F primer CCTGAGGAATGAGCGCTTTC, R primer GTTCAAACGTGCGTCTGCATC) were cloned by RT-PCR using cDNA synthesized from HH13/14 embryo mRNA. Full-length cDNAs were inserted into the pCAβ-IRES-GFP expression vector.

HEK293T cells were grown in DMEM (Gibco) + 10% fetal bovine serum (FBS), 1% GlutaMAX (Gibco) and 1% penicillin/streptomycin (Gibco), and transfected with appropriate expression vectors using polyethylenimine⁷¹. Pellets of 500 cells were made by recombining cells from individual transfections in a hanging drop culture⁷².

In vitro culture of explants. Tissues were excised from chicken and quail embryos as described above, and cultured *in vitro* for 24 or 48 h at 37 °C with 5% CO₂ on a 0.4 µm Nucleopore filter (Whatman, WHA110407) floating on DMEM (Gibco) with 10% FBS, 5% chicken embryo extract (US Biological), 1% GlutaMAX (Gibco) and 1% Penicillin/Streptomycin (Gibco)²⁹. Tissues were arranged such that the basal surface of the AIP faced the mesoderm explants. Spontaneous beating in 48 h explant co-cultures was recorded with a QImaging Retiga 2000R camera and QCapture Pro software.

Probes and antibodies. Whole-mount *in situ* hybridization and immunohistochemistry were performed as described^{73,74}. Probes used were as follows: *MYOCD* (ref. 43), *TBX5* (ref. 75), *IRX4* (ref. 26), *ISL1* (ref. 76), *PITX2* (ref. 77), *NXP1* (ref. 78), *NRP1* (ref. 79), *NOTO* (*cNOT1*) (ref. 80), *VTN* (ref. 81), *MOXD1* (*DBHR*) (ref. 82), *CXCL12* (*SDF1*) (ref. 83), *ID2* (ref. 84), *DLX6* (ref. 85) and *SHOX2* (ref. 86), kindly provided by the originating laboratories. *AMHC1* and *NKX2.5* were kindly provided by T. Brand and *GATA4* by B. Pain. The cDNA available for *VMHC1* (*MYH15*)²⁷ is a 2.5 kb cDNA, which also has significant (73%) homology to *MYH7b* (*Slow Myosin 2, SM2*); therefore, a short 0.6 kb probe (*VMHC1/MYH15*, generated after cutting with PstI, where the two sequences differ most) was used instead (see *VMHC1/MYH15* short in Supplementary Fig. 6). Other probes, including *MEF2C* (ChEST776g19), *NPPB* (*ANF*; ChEST509m15) and *GJA5* (*CX40*; ChEST304a4), were transcribed from EST clones (Supplementary Data 1)⁸⁷. Following whole-mount *in situ* hybridization, embryos were incubated in QCPN (Developmental Studies Hybridoma Bank, diluted 1:5) and/or anti-GFP antibody (Life Technologies, A11122, diluted 1:2,000); secondary antibodies used were goat anti-mouse IgG peroxidase (Jackson, 115-035-003), goat anti-rabbit IgG peroxidase (Santa Cruz, sc-2004) or goat anti-rabbit IgG alkaline phosphatase (Upstate, 12–448) diluted 1:1,000. Cryosections of 15 µm or paraffin sections of 10 µm were prepared. For skeletal staining, embryos were stained with Alcian Blue⁸⁸.

Scoring of co-cultures. Explant cultures (Supplementary Tables 1–6) were considered ‘positive’ if high-level expression was observed throughout the majority of the explant. The *n*-numbers in the figures represent those that were scored as positive. The *n*-numbers that include positive and patchy expression are indicated. Explants with no detectable expression or very weak expression (perhaps due to non-specific staining, constitutive expression and/or marginal induction) were scored as negative. Explants with high-level expression in a small patch (some of which could be due to contamination) were excluded from *P*-value calculations, unless indicated. To calculate *P* values, positive (plus patchy where specified) and negative counts were compared across two conditions (#3 alone versus #3 + AIP or #3 + Cont.) using two-tailed Fisher’s exact test with a 2 × 2 contingency table. *P* values ≤ 0.05 were deemed significant.

Data availability. The microarray data have been deposited in the ArrayExpress database under accession code E-MTAB-4048. All other data supporting the findings of this study are available within the article and its Supplementary information files or from the corresponding author upon reasonable request.

References

- Gurdon, J. B. Embryonic induction—molecular prospects. *Development* **99**, 285–306 (1987).
- Spemann, H. & Mangold, H. Über Induktion von Embryonalanlagen durch Implantation artfremder Organisatoren. *Roux’ Arch. EntwMech. Org.* **100**, 599–638 (1924).
- Anderson, C. & Stern, C. D. Organizers in development. *Curr. Top. Dev. Biol.* **117**, 435–454 (2016).
- Waddington, C. H. & Schmidt, G. A. Induction by heteroplastic grafts of the primitive streak in birds. *W. Roux Arch. Entwicklungsmech. Org.* **128**, 522–563 (1933).
- van Straaten, H. W., Hekking, J. W., Thors, F., Wiertz-Hoessels, E. L. & Drukker, J. Induction of an additional floor plate in the neural tube. *Acta Morphol. Neerl. Scand.* **23**, 91–97 (1985).
- Saunders, J. W. J. & Gasseling, M. T. in *Epithelial-Mesenchymal Interactions* (eds Fleischmeyer, R. & Billingham, R. E.) 78–97 (Williams & Wilkins, 1968).
- Martinez, S., Wassef, M. & Alvarado-Mallart, R. M. Induction of a mesencephalic phenotype in the 2-day-old chick prosencephalon is preceded by the early expression of the homeobox gene *en*. *Neuron* **6**, 971–981 (1991).
- Hornbruch, A. & Wolpert, L. Positional signalling by Hensen’s node when grafted to the chick limb bud. *J. Embryol. Exp. Morphol.* **94**, 257–265 (1986).
- Bellairs, R. Studies on the development of the foregut in the chick blastoderm. 1. The presumptive foregut area. *J. Embryol. Exp. Morph.* **1**, 115–124 (1953).
- Hamburger, V. & Hamilton, H. L. A series of normal stages in the development of the chick embryo. *J. Morphol.* **88**, 49–92 (1951).
- Storey, K. G., Crossley, J. M., De Robertis, E. M., Norris, W. E. & Stern, C. D. Neural induction and regionalisation in the chick embryo. *Development* **114**, 729–741 (1992).
- Wong, F. *et al.* eChickAtlas: an introduction to the database. *Genesis* **51**, 365–371 (2013).
- Lough, J. & Sugi, Y. Endoderm and heart development. *Dev. Dyn.* **217**, 327–342 (2000).
- Brand, T. Heart development: molecular insights into cardiac specification and early morphogenesis. *Dev. Biol.* **258**, 1–19 (2003).
- Pfister, S. *et al.* Sox17-dependent gene expression and early heart and gut development in Sox17-deficient mouse embryos. *Int. J. Dev. Biol.* **55**, 45–58 (2011).
- Kirby, M. L. *et al.* Hensen’s node gives rise to the ventral midline of the foregut: implications for organizing head and heart development. *Dev. Biol.* **253**, 175–188 (2003).
- Narita, N., Bielinska, M. & Wilson, D. B. Wild-type endoderm abrogates the ventral developmental defects associated with GATA-4 deficiency in the mouse. *Dev. Biol.* **189**, 270–274 (1997).
- Li, S., Zhou, D., Lu, M. M. & Morrisey, E. E. Advanced cardiac morphogenesis does not require heart tube fusion. *Science* **305**, 1619–1622 (2004).
- Varner, V. D. & Taber, L. A. Not just inductive: a crucial mechanical role for the endoderm during heart tube assembly. *Development* **139**, 1680–1690 (2012).
- Redkar, A., Montgomery, M. & Litvin, J. Fate map of early avian cardiac progenitor cells. *Development* **128**, 2269–2279 (2001).
- Rosenquist, G. C. A Radioautographic study of labelled grafts in the chick blastoderm. Development from primitive-streak stages to stage 12. *Contrib. Embryol. Carnegie Inst. Wash.* **38**, 71–110 (1966).
- Schultheiss, T. M., Burch, J. B. & Lassar, A. B. A role for bone morphogenetic proteins in the induction of cardiac myogenesis. *Genes Dev.* **11**, 451–462 (1997).
- Rosenquist, G. C. & DeHaan, R. L. Migration of precardiac cells in the chick embryo: a radioautographic study. *Contrib. Embryol. Carnegie Inst. Wash.* **38**, 111–121 (1966).
- Rawles, M. E. The heart-forming areas of the early chick blastoderm. *Physiol. Zool.* **16**, 22–43 (1943).
- Houweling, A. C., Somi, S., Van Den Hoff, M. J., Moorman, A. F. & Christoffels, V. M. Developmental pattern of ANF gene expression reveals a strict localization of cardiac chamber formation in chicken. *Anat. Rec.* **266**, 93–102 (2002).
- Bao, Z. Z., Bruneau, B. G., Seidman, J. G., Seidman, C. E. & Cepko, C. L. Regulation of chamber-specific gene expression in the developing heart by *Irx4*. *Science* **283**, 1161–1164 (1999).
- Bisaha, J. G. & Bader, D. Identification and characterization of a ventricular-specific avian myosin heavy chain, VMHC1: expression in differentiating cardiac and skeletal muscle. *Dev. Biol.* **148**, 355–364 (1991).
- Yutzey, K. E., Rhee, J. T. & Bader, D. Expression of the atrial-specific myosin heavy chain AMHC1 and the establishment of anteroposterior polarity in the developing chicken heart. *Development* **120**, 871–883 (1994).
- Schultheiss, T. M., Xydias, S. & Lassar, A. B. Induction of avian cardiac myogenesis by anterior endoderm. *Development* **121**, 4203–4214 (1995).
- Wang, G. F., Nikovits, W., Bao, Z. Z. & Stockdale, F. E. *Irx4* forms an inhibitory complex with the vitamin D and retinoic X receptors to regulate cardiac chamber-specific slow MyHC3 expression. *J. Biol. Chem.* **276**, 28835–28841 (2001).
- Wagner, M., Thaller, C., Jessell, T. & Eichele, G. Polarizing activity and retinoid synthesis in the floor plate of the neural tube. *Nature* **345**, 819–822 (1990).
- Lopez-Sanchez, C., Climent, V., Schoenwolf, G. C., Alvarez, I. S. & Garcia-Martinez, V. Induction of cardiogenesis by Hensen’s node and fibroblast growth factors. *Cell. Tissue. Res.* **309**, 237–249 (2002).
- Streit, A. *et al.* Preventing the loss of competence for neural induction: HGF/SF, L5 and Sox-2. *Development* **124**, 1191–1202 (1997).
- Alsan, B. H. & Schultheiss, T. M. Regulation of avian cardiogenesis by Fgf8 signaling. *Development* **129**, 1935–1943 (2002).
- Linker, C. & Stern, C. D. Neural induction requires BMP inhibition only as a late step, and involves signals other than FGF and Wnt antagonists. *Development* **131**, 5671–5681 (2004).
- Pinho, S. *et al.* Distinct steps of neural induction revealed by Asterix, Obelix and TrkC, genes induced by different signals from the organizer. *PLoS ONE* **6**, e19157 (2011).
- Tickle, C. The number of polarizing region cells required to specify additional digits in the developing chick wing. *Nature* **289**, 295–298 (1981).
- Streit, A., Berliner, A. J., Papanayotou, C., Sirulnik, A. & Stern, C. D. Initiation of neural induction by FGF signalling before gastrulation. *Nature* **406**, 74–78 (2000).
- Crossley, P. H., Martinez, S. & Martin, G. R. Midbrain development induced by FGF8 in the chick embryo. *Nature* **380**, 66–68 (1996).
- Echelard, Y. *et al.* Sonic hedgehog, a member of a family of putative signaling molecules, is implicated in the regulation of CNS polarity. *Cell* **75**, 1417–1430 (1993).
- Riddle, R. D., Johnson, R. L., Laufer, E. & Tabin, C. Sonic hedgehog mediates the polarizing activity of the ZPA. *Cell* **75**, 1401–1416 (1993).
- Zhang, X. M., Ramalho-Santos, M. & McMahon, A. P. Smoothed mutants reveal redundant roles for Shh and Ihh signaling including regulation of L/R asymmetry by the mouse node. *Cell* **105**, 781–792 (2001).
- Warkman, A. S., Yatskevych, T. A., Hardy, K. M., Krieg, P. A. & Antin, P. B. Myocardin expression during avian embryonic heart development requires the endoderm but is independent of BMP signaling. *Dev. Dyn.* **237**, 216–221 (2008).
- Orts-Llorca, F. Influence of the endoderm on heart differentiation during the early stages of development of the chicken embryo. *Roux’ Arch. EntwMech.* **154**, 533–551 (1963).
- Orts-Llorca, F. Influence of the endoderm on heart differentiation. *Roux’ Arch. EntwMech.* **156**, 368–370 (1965).
- Yamazaki, Y. & Hirakow, R. Factors required for differentiation of chick precardiac mesoderm cultured invitro. *Proc. Jpn Acad. B-Phys.* **67**, 165–169 (1991).
- Sugi, Y. & Lough, J. Anterior endoderm is a specific effector of terminal cardiac myocyte differentiation of cells from the embryonic heart forming region. *Dev. Dyn.* **200**, 155–162 (1994).
- Gannon, M. & Bader, D. Initiation of cardiac differentiation occurs in the absence of anterior endoderm. *Development* **121**, 2439–2450 (1995).
- Marvin, M. J., Di Rocco, G., Gardiner, A., Bush, S. M. & Lassar, A. B. Inhibition of Wnt activity induces heart formation from posterior mesoderm. *Genes Dev.* **15**, 316–327 (2001).
- Lough, J. *et al.* Combined BMP-2 and FGF-4, but neither factor alone, induces cardiogenesis in non-precordiac embryonic mesoderm. *Dev. Biol.* **178**, 198–202 (1996).
- Schlange, T., Andree, B., Arnold, H. H. & Brand, T. BMP2 is required for early heart development during a distinct time period. *Mech. Dev.* **91**, 259–270 (2000).

52. Andree, B., Duprez, D., Vorbusch, B., Arnold, H. H. & Brand, T. BMP-2 induces ectopic expression of cardiac lineage markers and interferes with somite formation in chicken embryos. *Mech. Dev.* **70**, 119–131 (1998).
53. Barron, M., Gao, M. & Lough, J. Requirement for BMP and FGF signaling during cardiogenic induction in non-precordial mesoderm is specific, transient, and cooperative. *Dev. Dyn.* **218**, 383–393 (2000).
54. Jiang, Y., Tarzami, S., Burch, J. B. & Evans, T. Common role for each of the cGATA-4/5/6 genes in the regulation of cardiac morphogenesis. *Dev. Genet.* **22**, 263–277 (1998).
55. Bellairs, R. Studies on the development of the foregut in the chick blastoderm. 2. The morphogenetic movements. *J. Embryol. Exp. Morphol.* **1**, 369–385 (1953).
56. Kimura, W., Yasugi, S., Stern, C. D. & Fukuda, K. Fate and plasticity of the endoderm in the early chick embryo. *Dev. Biol.* **289**, 283–295 (2006).
57. Hochgreb, T. *et al.* A caudorostral wave of RALDH2 conveys anteroposterior information to the cardiac field. *Development* **130**, 5363–5374 (2003).
58. Orts-Llorca, F., Collado, J. J. & Dehaan, R. L. Determination of heart polarity (arterio venous axis) in the chicken embryo. *W. Roux Arch. Entwicklungsmech. Org.* **158**, 147–163 (1967).
59. Heine, U. I., Roberts, A. B., Munoz, E. F., Roche, N. S. & Sporn, M. B. Effects of retinoid deficiency on the development of the heart and vascular system of the quail embryo. *Virchows. Arch. B. Cell. Pathol. Incl. Mol. Pathol.* **50**, 135–152 (1985).
60. Stalsberg, H. & DeHaan, R. L. Endodermal movements during foregut formation in the chick embryo. *Dev. Biol.* **18**, 198–215 (1968).
61. Joubin, K. & Stern, C. D. Molecular interactions continuously define the organizer during the cell movements of gastrulation. *Cell* **98**, 559–571 (1999).
62. Selleck, M. A. & Stern, C. D. Fate mapping and cell lineage analysis of Hensen's node in the chick embryo. *Development* **112**, 615–626 (1991).
63. Harfe, B. D. *et al.* Evidence for an expansion-based temporal Shh gradient in specifying vertebrate digit identities. *Cell* **118**, 517–528 (2004).
64. Bangs, F. *et al.* Identification of genes downstream of the Shh signalling in the developing chick wing and syn-expressed with Hoxd13 using microarray and 3D computational analysis. *Mech. Dev.* **127**, 428–441 (2010).
65. Affymetrix. Guide to probe logarithmic error (PLIER) estimation. http://media.affymetrix.com/support/technical/notes/plier_technote.pdf (2005).
66. Talloen, W. *et al.* I/NI-calls for the exclusion of non-informative genes: a highly effective filtering tool for microarray data. *Bioinformatics* **23**, 2897–2902 (2007).
67. Sang, H. Prospects for transgenesis in the chick. *Mech. Dev.* **121**, 1179–1186 (2004).
68. New, D. A. T. A new technique for the cultivation of the chick embryo *in vitro*. *J. Embryol. Exp. Morphol.* **3**, 320–332 (1955).
69. Stern, C. D. & Ireland, G. W. An integrated experimental study of endoderm formation in avian embryos. *Anat. Embryol.* **163**, 245–263 (1981).
70. Tickle, C. Grafting of apical ridge and polarizing region. *Methods Mol. Biol.* **97**, 281–291 (1999).
71. Boussif, O. *et al.* A versatile vector for gene and oligonucleotide transfer into cells in culture and *in vivo*: polyethylenimine. *Proc. Natl Acad. Sci. USA* **92**, 7297–7301 (1995).
72. Streit, A. & Stern, C. D. Mesoderm patterning and somite formation during node regression: differential effects of chordin and noggin. *Mech. Dev.* **85**, 85–96 (1999).
73. Streit, A. & Stern, C. D. Combined whole-mount *in situ* hybridization and immunohistochemistry in avian embryos. *Methods* **23**, 339–344 (2001).
74. Stern, C. D. Detection of multiple gene products simultaneously by *in situ* hybridization and immunohistochemistry in whole mounts of avian embryos. *Curr. Top. Dev. Biol.* **36**, 223–243 (1998).
75. Isaac, A. *et al.* Tbx genes and limb identity in chick embryo development. *Development* **125**, 1867–1875 (1998).
76. Pfaff, S. L., Mendelsohn, M., Stewart, C. L., Edlund, T. & Jessell, T. M. Requirement for LIM homeobox gene *Isl1* in motor neuron generation reveals a motor neuron-dependent step in interneuron differentiation. *Cell* **84**, 309–320 (1996).
77. Logan, M., Pagan-Westphal, S. M., Smith, D. M., Paganessi, L. & Tabin, C. J. The transcription factor *Pitx2* mediates situs-specific morphogenesis in response to left-right asymmetric signals. *Cell* **94**, 307–317 (1998).
78. Apostolova, G. *et al.* Neurotransmitter phenotype-specific expression changes in developing sympathetic neurons. *Mol. Cell. Neurosci.* **35**, 397–408 (2007).
79. Herzog, Y., Kalcheim, C., Kahane, N., Reshef, R. & Neufeld, G. Differential expression of neuropilin-1 and neuropilin-2 in arteries and veins. *Mech. Dev.* **109**, 115–119 (2001).
80. Stein, S., Niss, K. & Kessel, M. Differential activation of the clustered homeobox genes *CNOT2* and *CNOT1* during notogenesis in the chick. *Dev. Biol.* **180**, 519–533 (1996).
81. Pons, S. & Marti, E. Sonic hedgehog synergizes with the extracellular matrix protein vitronectin to induce spinal motor neuron differentiation. *Development* **127**, 333–342 (2000).
82. Knecht, A. K. & Bronner-Fraser, M. DBHR, a gene with homology to dopamine beta-hydroxylase, is expressed in the neural crest throughout early development. *Dev. Biol.* **234**, 365–375 (2001).
83. Rehimi, R. *et al.* Stromal-derived factor-1 (SDF-1) expression during early chick development. *Int. J. Dev. Biol.* **52**, 87–92 (2008).
84. Martinsen, B. J. & Bronner-Fraser, M. Neural crest specification regulated by the helix-loop-helix repressor *Id2*. *Science* **281**, 988–991 (1998).
85. Hsu, S. H. *et al.* *Dlx5*- and *Dlx6*-mediated chondrogenesis: differential domain requirements for a conserved function. *Mech. Dev.* **123**, 819–830 (2006).
86. Tiecke, E. *et al.* Expression of the short stature homeobox gene *Shox* is restricted by proximal and distal signals in chick limb buds and affects the length of skeletal elements. *Dev. Biol.* **298**, 585–596 (2006).
87. Boardman, P. E. *et al.* A comprehensive collection of chicken cDNAs. *Curr. Biol.* **12**, 1965–1969 (2002).
88. McLeod, M. J. Differential staining of cartilage and bone in whole mouse fetuses by alcian blue and alizarin red S. *Teratology* **22**, 299–301 (1980).

Acknowledgements

This study was funded by BBSRC and ERC. We thank Angel Pang, Jiahui Liu, Andrew Bain, Monique Welten and Lynn McTeir for help with *in situ* hybridization, Megan Davey for comments on the manuscript, Duncan Davidson for an anatomical ontology, Michael Wicks for enhancing the eChickAtlas database, Federica Bertocchini for tissue collection, Melanie Krause for help with cell pellet grafts and Irene de Almeida for help with cloning.

Author contributions

M.A.F.K. produced the Venn diagrams and heatmap. F.W., D.W.B. and M.A.F.K. analysed the microarray data. T.S. performed some of the limb stage *in situ* hybridizations and cloned the VTN expression plasmid. N.M.M.O. performed cell transfections and generated the cell pellets. C.D.S., D.W.B., C.T. and R.A.B. conceived the project and obtained funding. C.T. performed the limb stage tissue collections. C.A. performed all other experiments. C.D.S. designed the screen, performed the Boolean comparisons and participated in the analysis of other data. C.A. and C.D.S. wrote the manuscript.

Additional information

Supplementary Information accompanies this paper at <http://www.nature.com/naturecommunications>

Competing financial interests: The authors declare no competing financial interest.

Reprints and permission information is available online at <http://npg.nature.com/reprintsandpermissions/>

How to cite this article: Anderson, C. *et al.* A strategy to discover new organizers identifies a putative heart organizer. *Nat. Commun.* **7**:12656 doi: 10.1038/ncomms12656 (2016).



This work is licensed under a Creative Commons Attribution 4.0 International License. The images or other third party material in this article are included in the article's Creative Commons license, unless indicated otherwise in the credit line; if the material is not included under the Creative Commons license, users will need to obtain permission from the license holder to reproduce the material. To view a copy of this license, visit <http://creativecommons.org/licenses/by/4.0/>

© The Author(s) 2016